Available online at www.sciencedirect.com
ScienceDirect
Building and Environment 43 (2008) 238–245
BUILDING AND ENVIRONMENT
www.elsevier.com/locate/buildenv

Influence of fins on formaldehyde removal in annular photocatalytic reactors

Jinhan Mo, Yinping Zhang*, Rui Yang, Qiujian Xu

Department of Building Science, Tsinghua University, Beijing 100084, PR China

Received 23 October 2005; received in revised form 23 November 2005; accepted 13 December 2005

Abstract

The influence of fins on formaldehyde removal in annular photocatalytic reactors was theoretically, numerically and experimentally studied. The simulated and experimental results agreed well. It was found that mass transfer tends to be the bottleneck of formaldehyde removal in conventional annular photocatalytic oxidation (PCO) reactors. When using fins coated with titania in a PCO reactor, the reaction area is greatly increased and the convective mass transfer is, therefore, obviously enhanced. The reaction coefficient may, however, be reduced. On the whole, the formaldehyde removal performance in an annular PCO reactor can be obviously improved by adding fins to the reactor. This analysis is helpful for annular PCO reactor design, and for performance optimization.

Keywords: Volatile organic compounds; Titania; Photocatalytic oxidation; Mass transfer

1. Introduction

In recent decades, buildings have been more tightly sealed so as to reduce the energy consumption associated with indoor air-conditioning. Meanwhile, with the increasing use of synthetic building materials and furnishings that emit volatile organic compounds (VOCs), the VOC concentrations in indoor air tend to be higher than those allowed by existing codes [1,2]. High VOC concentrations indoors are known to be harmful to human health [3–7]. Formaldehyde, a typical indoor air chemical pollutant emitted from furniture and decorating materials, is found to be associated with asthma, masopharyngeal cancer and multiple subjective health complaints [8]. Many researchers have developed new advanced technologies to quickly and economically remove VOCs from indoor air. Photocatalytic oxidation (PCO) is an innovative and a promising approach among them [9–11].

VOC removal by PCO is a surface reaction process consisting of two important steps: mass transfer of VOCs to the reaction surface and decomposition of the VOC by the photocatalyst. Thus, the VOC convective mass transfer rate, the reaction rate and the reaction surface area are the most important factors influencing VOC removal in a PCO reactor. These factors are related to many other factors such as the reactor geometry, the airflow velocity, the physical properties of the VOC species, the wavelength and intensity of the UV irradiation, and photocatalyst performances etc.

Many physical models of PCO reactors have been developed. It is assumed that the gas-phase absorption, scattering, and reflection of UV light is negligible and the light reflection from the photocatalyst coating diffuses perfectly. Hall et al. [12] developed a reduced order model for photocatalytic honeycomb reactors, and discussed mass transport and reaction rate limits. They found that the product of volumetric flow rate and conversion rate, which represents the overall VOC removal rate, reached an asymptote with the increased velocity. Zhang et al. [13] developed a PCO reactor model based on the mass transfer analysis, and found that two parameters, the number of the mass transfer unit, NTU_m, and the fractional conversion, ε, are the main parameters influencing the photooxidation performance of a PCO reactor. In the model, it was assumed that the photocatalytic reaction was a first-order

*Corresponding author.
E-mail address: zhangyp@mail.tsinghua.edu.cn (Y. Zhang).

0360-1323/$ - see front matter © 2006 Elsevier Ltd. All rights reserved.
doi:10.1016/j.buildenv.2005.12.027

reaction with a constant reaction rate coefficient and a constant convective mass transfer coefficient along the flow direction. Based on Zhang's model, Yang et al. [14] improved this model and defined the reaction effectiveness, η, to determine the bottleneck of VOC removal in PCO reactors. Mo et al. [15] presented a novel insight into VOC removal in PCO reactors: (1) the mass transfer unit, NTU_m, is the product of three dimensionless parameters (the ratio of the reaction area to the cross-sectional area of the flow channel, A^*, the Stanton number of mass transfer, St_m and the reaction effectiveness, η); (2) the intersection angle between velocity and the concentration gradient of fluid flow, β, describes the synergistic degree of velocity and concentration fields and strongly influences the convective mass transfer coefficient. This insight is useful in PCO reactor design and performance optimization.

In practice, three types of PCO reactors (plate, honeycomb and annular) are usually applied. A plate reactor is frequently used in experiments to generate oxidation rate data for VOC removal, while the honeycomb and annular reactors are commonly applied to indoor air purification. For the honeycomb reactor, it is known that the UV radiation intensity drops sharply with increasing distance into the channel [16]. For an annular reactor, the mass transfer rate is smaller than that of the honeycomb [15], while the radiation intensity is uniform along the tube.

In the present study, a method for evaluating the effectiveness of VOC removal in a PCO reactor was introduced. Based on this study, the VOC removal bottleneck of the annular PCO reactor was numerically studied, and was validated by the experimental results. The prediction and evaluation of the VOC removal performance of this type of reactor with fins was made.

2. Key parameters for analyzing reactor performance

The key parameters of a PCO reactor are the fractional conversion of VOC, ε [13], and the VOC removal rate [12], $\dot{m}$. They are expressed as follows [15]:

$$\varepsilon = \frac{C_{in} - C_{out}}{C_{in}} = 1 - e^{-NTU_m}, \quad (1)$$

$$NTU_m = A^* St_m \eta,$$

$$A^* = \frac{A_r}{A_c}, \quad (2)$$

$$\dot{m} = GC_{in}\varepsilon = GC_{in}(1 - e^{-NTU_m}), \quad (3)$$

where C_{in} and C_{out} are the inlet and outlet VOC concentrations of a PCO reactor, respectively, mol/m^3; NTU_m is the number of the mass transfer unit; G is the volumetric airflow rate, m^3/s.

A^* represents the geometric and structural characteristics of a PCO reactor. St_m is the dimensionless convective mass transfer coefficient and shows the synergistic degree of alignment between the velocity and concentration fields. η describes the relative intensity between the PCO reaction rate and the mass transfer rate. Both of St_m and η are positive and not greater than 1. The VOC removal bottleneck of the PCO reactor can be determined by analyzing the value of A^*, St_m, and η. In order to force the actual conversion to be greater than a desired value, ε_d ($\varepsilon_d < 1$, for example 90%), the value of A^* should be greater than the desired NTU_m,

$$A^* \geqslant NTU_{m,d} = -\ln(1 - \varepsilon_d). \quad (4)$$

If not, no matter how great St_m and η are, the actual conversion will be less than ε_d. In other words, for this case ($A^* < NTU_{m,d}$), A^* is the bottleneck to improving VOC removal performance of a PCO reactor. Therefore, for a PCO reactor's geometric dimension design or selection, only the structure with A^* greater than $NTU_{m,d}$ can be a candidate.

However, $A^* \geqslant NTU_{m,d}$ is not sufficient. Be sure that

$$A^* St_m \geqslant NTU_{m,d}. \quad (5)$$

If $St_m < NTU_{m,d}$, then St_m is the bottleneck to improving the performance of VOC removal.

If ($A^* St_m$) is adequately high, be sure that

$$A^* St_m \eta \geqslant NTU_{m,d}. \quad (6)$$

Otherwise, η is the bottleneck.

By using this method, the bottleneck to VOC removal performance can be determined. If every step is satisfied, the reactor is promising.

A^* only depends on the geometric size of the PCO reactor [15]. St_m and η can be calculated using a CFD analysis.

3. Experimental details

The formaldehyde removal performance of two kinds of annular PCO reactors designed by us (Fig. 1(a) without fins and (b) with six fins), were measured in a gas-tight stainless steel chamber ($1.2 \times 1.2 \times 1.2\,m^3$) with no VOC sources or sinks (Fig. 2). The tubes used in the experiments had an inner diameter of 48 mm and a length of 265 mm. The UV lamp's external diameter was 15 mm and its length was the same as the tube, with 98% of the UV lamp radiation emitted at 254 nm and a UV radiation intensity of $4.54\,mW/cm^2$ on the lamp surface. The UV radiation intensity was measured by a UVC power meter with the sensor being close to the lamp surface tightly. An axial flow fan installed in the stainless steel chamber ensured that the formaldehyde was uniformly distributed. A centrifugal fan supplied the required airflow rate for the reactor. The air temperature was controlled at $25 \pm 0.5\,^{\circ}C$ by using an electric heater on the bottom of the chamber. The initial formaldehyde and water vapor concentrations inside the chamber were generated by injection and evaporation, respectively.

The mass conservation equation for formaldehyde in the chamber together with the initial condition can be

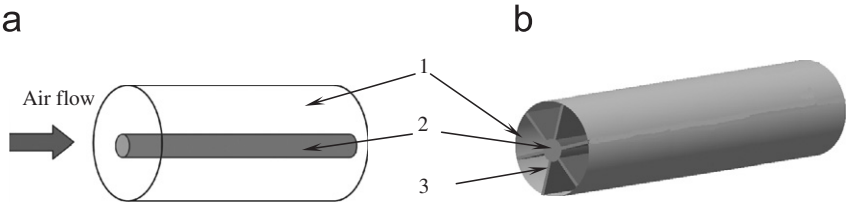

Fig. 1. Schematic of the annular reactor (a) without fins and (b) with fins: (1) inner surface of exterior cylinder coated with nanometer TiO_2 powders; (2) UV lamp and (3) rectangular fins.

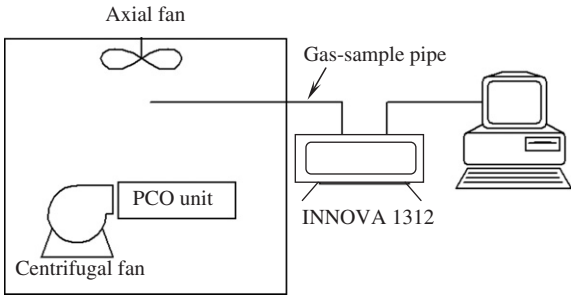

Fig. 2. Schematic of the gas-tight stainless steel chamber and formaldehyde concentration measurement system.

written as [14]:

$$-V\frac{dC}{dt} = GC(t)(1-e^{-NTU_m}),$$
$$t=0, \quad C(t)=C_{ini}, \tag{7}$$

where V is the chamber volume, m^3 and C_{ini} is the initial concentration of formaldehyde in chamber, ppm_v.

The solution of Eq. (7) is

$$\ln C(t) = \ln C_{ini} - \frac{G}{V}(1-e^{-NTU_m})t. \tag{8}$$

The fractional conversion (or NTU_m) was calculated from the slope of the line fit to the experimental data plotted as $\ln(C(t))$ versus t using the least-squares method.

Formaldehyde concentrations in the chamber were measured by using a gas analyzer (INNOVA 1312) and a data log system. The volumetric airflow rate through the PCO reactor was measured by an anemometer.

4. Numerical analysis

The mass transfer and PCO of formaldehyde were simulated by solving the mass transfer equation for the reactor. The radiation transport equation was applied to describe the UV light intensity in the PCO reactor, which was important for the reaction boundary condition.

The velocity and VOC distribution in the reactor were calculated by the CFD method. Considering the symmetric nature of the structure inside the reactor with fins, only one channel was taken into consideration (Fig. 3).

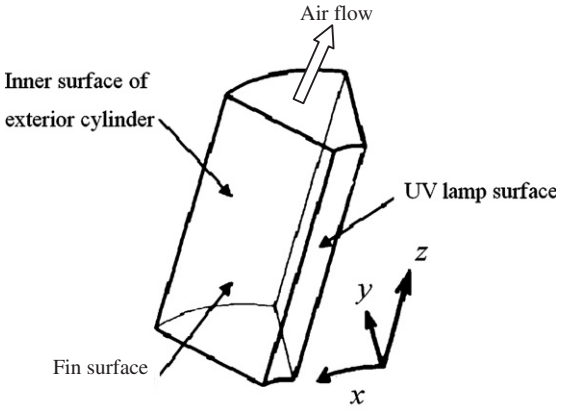

Fig. 3. Schematic of the coordinate system for a single channel in the reactor with fins (x-arc distance, y-radial distance and z-axial distance).

4.1. Radiation transport equation

It is seen from Fig. 1 that the UV radiation flux on the reaction surface was not uniform. Reasonably, to simplify the radiation transport analysis, the assumptions in Ref. [16] were:

(1) The channel of the tube reactor was identically irradiated internally by a lamp, which emits primarily at the wavelength of 254 nm.
(2) Gas-phase absorption, scattering, and reflection of the light were negligible.
(3) All the thermal radiative properties (absorptance α and reflectance ρ) were assumed to be independent of the light incidence angle.
(4) The photocatalytic coating on the internal wall of the tube was uniform, opaque, diffuse and gray. Thus, $\alpha_\lambda + \rho_\lambda = 1$ and the emissivity $\varepsilon_\lambda = \alpha_\lambda$.
(5) The photocatalytic coating did not emit radiation in the spectral region of interest.

There is a radiation balance on a reaction surface consisting of three parts: the incident UV flux, G, mW/cm^2; the total emission UV flux, J, mW/cm^2; and the absorbed radiation, q, mW (Fig. 4(a)). For surface i, there is

$$q_i = A_i(G_i - J_i), \tag{9}$$

where A_i represents the area of surface i. Fig. 4(b) shows that the total UV emission flux of surface i consists of the emission radiation, E, and the reflected part of the incident

radiation, ρG, which is,

$$J_i = E_i + \rho_{\lambda,i} G_i = \varepsilon_{\lambda,i} E_{b,i} + \rho_{\lambda,i} G_i. \quad (10)$$

Recognizing that $\rho_{\lambda,i} = 1 - \alpha_{\lambda,i} = 1 - \varepsilon_{\lambda,i}$ for an opaque, diffuse, gray surface, it yields

$$J_i = \varepsilon_{\lambda,i} E_{b,i} + (1 - \varepsilon_{\lambda,i}) G_i. \quad (11)$$

Combining Eqs. (7)–(9), we obtain

$$q_i = \frac{J_i - E_{b,i}}{(1 - \varepsilon_{\lambda,i})/\varepsilon_{\lambda,i} A_i}. \quad (12)$$

In a multi-surface-radiant-system, we have [17]

$$q_i = \frac{J_i - E_{b,i}}{(1 - \varepsilon_{\lambda,i})/\varepsilon_{\lambda,i} A_i} = \sum_{j=1}^{N} \frac{J_j - J_i}{(A_i F_{ij})^{-1}}. \quad (13)$$

With the following reciprocal relationship

$$F_{ji} A_j = F_{ij} A_i. \quad (14)$$

We have

$$J_i = \varepsilon_{\lambda,i} E_{b,i} + (1 - \varepsilon_{\lambda,i}) \sum_{j=1}^{N} J_j F_{ij}, \quad (15)$$

where N is the total number of all the differential surfaces including the light source and the reaction surfaces; F_{ij} is the view factor of surface from i to j. The view factor between two finite surfaces is expressed as

$$F_{ij} = \frac{\cos \varphi_i \cos \varphi_j}{\pi r^2} A_j, \quad (16)$$

where r represents the distance between the centroids of surfaces i and j; φ_i is the intersection angle between the normal direction of surface i, and the straight line through the centroids of surface i and j.

The geometric relationship of i and j surfaces in the annular channel is shown in Fig. 5.

By solving Eq. (15), the total emission radiation, J is calculated. Therefore, the absorbed radiation, q can be obtained. The UV radiation intensity on the reaction surface, I_{Wall}, can be expressed as follows:

$$I_{Wall} = q/A. \quad (17)$$

The dimensionless UV radiation intensity, I^+ is defined as follows:

$$I^+ = \frac{I_{Wall}}{I_{Lamp}}, \quad (18)$$

where, I_{Lamp} is the UV radiation intensity on the surface of the UV lamp, mW/cm^2.

In addition, the reflectance ρ is light-wavelength dependent. Brucato et al. [18] presented an empirical reflectivity expression. For that,

$$\rho(\lambda) = 0.515 + 0.455 \tanh\left[\left(\frac{\lambda - 420}{20}\right) + 1.85\right]. \quad (19)$$

For $\lambda = 254\,nm$, ρ is equal to 0.055.

4.2. Velocity and concentration field

For the case where the air temperature changes little, the air properties can be regarded as constant. Therefore, we have the following governing equations:

Continuity equation:

$$\nabla \cdot (\vec{v}) = 0. \quad (20)$$

Momentum equation:

$$\vec{v} \cdot \nabla \vec{v} = -\nabla p + \mu \nabla^2 \vec{v}. \quad (21)$$

Conservation equation for formaldehyde species concentration C:

$$\vec{v} \cdot \nabla C = D \nabla^2 \vec{v}. \quad (22)$$

In Eqs. (20)–(22), is the velocity, m/s; p the pressure, Pa; μ the dynamic viscosity, kg/(ms); C the formaldehyde concentration, ppm_v; D the diffusion coefficient of formaldehyde in air, m^2/s.

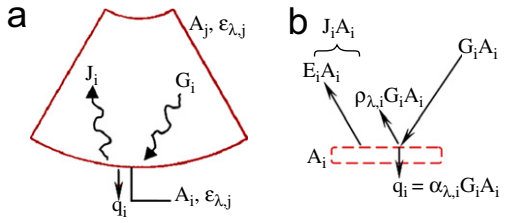

Fig. 4. Radiation exchange in a reactor with fins: (a) schematic of the channel and (b) radiation balance corresponding to Eq. (10).

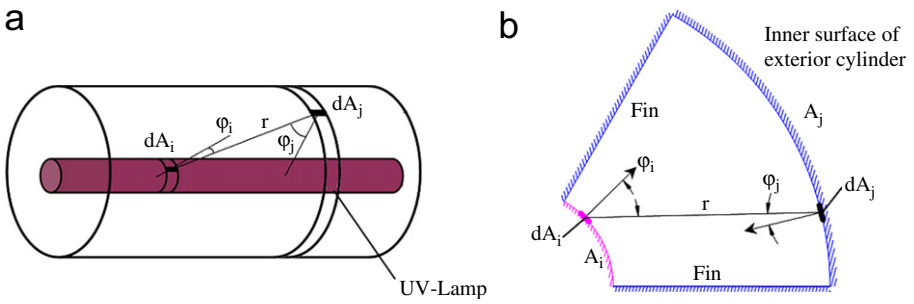

Fig. 5. Schematic of the geometric relationship between the differential areas of dA_i and dA_j in an annular channel for the view factor calculation: (a) without fins and (b) with fins.

The PCO reaction occurs at the surfaces coated with nanometer TiO_2 powders.

The boundary conditions of Eqs. (20)–(22) are:

At the inlet,

$$u_x = u_y = 0, \quad u_z = \text{const}, \quad C = \text{const}. \tag{23}$$

At the walls,

$$u_x = u_y = u_z = 0. \tag{24}$$

At the non-reaction surface,

$$\frac{\partial C}{\partial \vec{n}} = 0. \tag{25}$$

At the reaction surface,

$$-D \left.\frac{\partial C}{\partial \vec{n}}\right|_{\text{wall}} = \Re, \tag{26}$$

where $\Re$ is the local heterogeneous reaction rate. It can be expressed by the Langmuir–Hinshelwood–Hougen–Watson kinetic-rate form [19]:

$$\Re(C_S, C_W, I_G, I_{Wall}) = K_0 \left(\frac{K_1 C_S}{1 + K_1 C_S + K_2 C_W}\right) \times \left(\frac{K_4 C_W}{1 + K_3 C_S + K_4 C_W}\right) \left(\frac{I_{Wall}}{I_G}\right)^n, \tag{27}$$

where, K_0 ($\mu mol^{-1}/cm^2/h$) is the rate constant for a given UV radiation intensity, I_G, mW/cm^2; K_1, K_2, K_3, K_4 ($ppmv^{-1}$) are the Langmuir adsorption equilibrium constants; and C_S (ppmv) and C_W (ppmv) are the gas-phase concentrations of formaldehyde and water vapor on the surface, respectively.

In simulation, I_{wall} is imported into Fluent as part of the boundary conditions of concentration. Using fluent, the velocity and concentration distributions can be predicted. The standard k–e turbulence model was applied. The algorithm of SIMPLE was used to uncouple the pressure and velocity. The QUICK format was used during the simulation. The turbulence intensity was set as 5%. The turbulence kinetic energy and turbulence dissipation rate were set as 0.07 and 0.01, respectively.

5. Results and discussion

5.1. Influence of fins on radiation field

Fig. 6 shows the predicted UV radiation intensity profile for the annular PCO reactor without fins. The UV radiation intensity is nearly uniform increasing with distance into the channel except for the channel ends. However, for the reactor with fins, the UV radiation intensity distribution on the reaction surface is not uniform, in particular on the fins. For a reactor with six fins, Fig. 7 shows the dimensionless UV radiation intensity on the internal surfaces of the exterior cylinder and the fins (see Fig. 3 for geometry details). It is seen that the UV radiation intensity on the internal surface of the exterior cylinder is comparatively uniform, but in the y direction, the UV radiation intensity decreases sharply.

5.2. Comparison of CFD-predicted and experimental results

Fig. 8 shows the experimental photocatalytic reaction data for formaldehyde. The volumetric airflow rate through a single tube was 25.0 m^3/h. The initial formaldehyde concentration in the test was 1.50 ppmv. The formaldehyde removal performance of the reactor with fins was obviously better than that of the reactor without fins. From Fig. 8(b), it is seen that the slope of the line-fitting experimental data is approximately constant. That

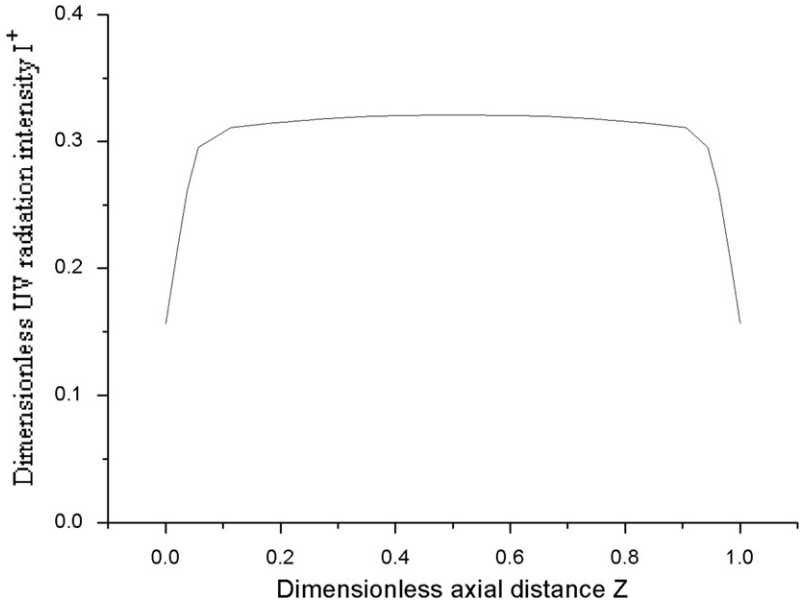

Fig. 6. Dimensionless UV radiation intensity on the surfaces of annular PCO reactor with fins.

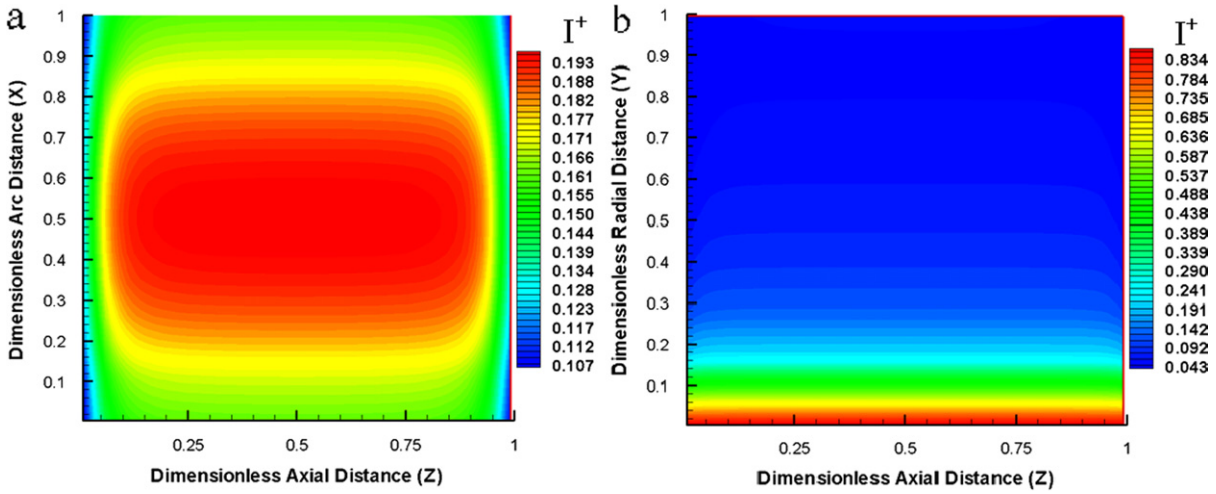

Fig. 7. Dimensionless UV radiation intensity on the surfaces of (a) the exterior cylinder and (b) the fins with I_{Lamp} 4.5 mW/cm^2 ($X = x/Lx$, $Y = y/Ly$, $Z = z/Lz$. Lx, Ly, Lz are the length in x-, y- and z-direction, respectively).

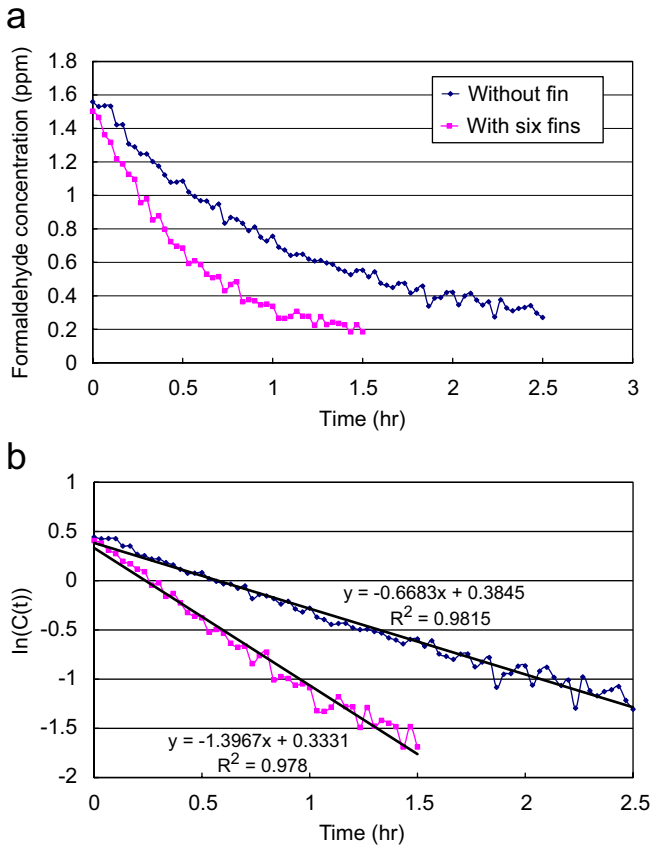

Fig. 8. Experimental photocatalytic reaction data for formaldehyde: (a) concentration decay curve and (b) ln($C(t)$) versus testing time.

means ε can be regarded as constant, which is the same as Yang's result [14].

Table 1 shows a comparison of the experimental data with the CFD-predicted results for the annular reactors with six fins and without fins. It can be seen that the relative difference between the CFD-predicted results and the experimental data is very small, which means that this CFD model is capable of predicting the experimental results with a high level of confidence.

5.3. Influence of fins on formaldehyde removal performance

Comparing Figs. 6 and 7, it can be concluded that the UV radiation intensity is reduced almost 50% on the internal surface of the exterior cylinder. However, the fractional conversion increases about 70% compared to the reactor without fins. It is necessary to further understand the influence of fins on the formaldehyde removal performance.

Assuming that the desired fractional conversion is 30%, corresponding to Eq. (1), NTU_m has to be greater than 0.36. According to the discussion in Section 2 (from Eqs. (4)–(6)), the formaldehyde removal performance can be evaluated step-by-step. From Table 1, it is known that A^* is always greater than 0.36. Thus, the geometry design for this type of PCO reactor is adequate in the reaction area. However, the product of A^* and St_m is much less than 0.36, which means that the final fractional conversion is not satisfactory. This implies that the bottleneck of an annular PCO reactor is the mass transfer rate. If fins are applied, A^* and St_m are both enhanced, while η decreases simultaneously.

Fig. 9 shows the CFD-predicted results of the reactors with various fins. The fractional conversion, ε, monotonically increases with increasing fin number. When the number of fins is less than 12, the term, (A^*St_m), is less than 0.36. That is to say, if more than 30% of the fractional conversion is required, more than 12 fins have to be applied into this type PCO reactor. The formaldehyde removal bottleneck is changed from the mass transfer rate to the reaction rate, when the number of fins is increased. For example, if 12 fins are applied, (A^*St_m) is greater than 0.36, but η is less than 40%, which means that the reaction rate is

Table 1
The formaldehyde removal performances of two kinds of annular reactors: with fins and without fins

PCO reactor	Measured ε (%)	Predicted ε (%)	Diff. (%)	NTU_m ($\times 10^{-2}$)	A^*	St_m ($\times 10^{-3}$)	η (%)
With six fins	9.40	10.2	7.8	9.87	56.6	3.20	54.7
Without fins	5.42	6.10	11.1	5.57	24.5	2.97	76.6

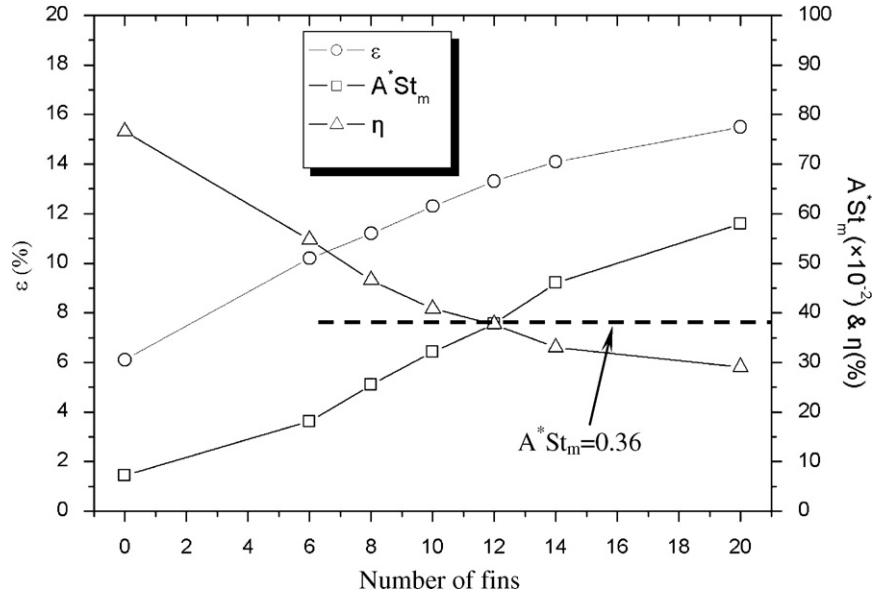

Fig. 9. ε, (A^*St_m), and η versus the number of fins in the annular PCO reactor.

less than the mass transfer rate. Thus, in this case, the question of how to enhance the reaction rate should be taken into account after fins were used.

In summary, using fins will increase the reaction area and mass transfer rate and offset the decreasing of η of an annular PCO reactor. The analysis of the influence of fins is also useful for other PCO reactor design, optimization and control.

6. Conclusions

(1) The CFD analysis validated with experiments was helpful in predicting the formaldehyde removal performance of the annular PCO reactor.
(2) ε, A^* and St_m increase with an increasing number of fins, while η decreases.
(3) The formaldehyde removal bottleneck in the annular PCO reactor is the mass transfer rate. Applying fins is effective in improving the value of (A^*St_m). However, as more fins are added, the reaction rate gradually becomes the bottleneck.
(4) The analysis is helpful for various PCO reactor designs, optimization and control.

Acknowledgments

This work was supported by the National Nature Science Foundation of China (Grant nos.: 50276033 and 50436040).

References

[1] US EPA. Sick building syndrome (SBS), indoor air facts no. 4 (revised), U.S. Environmental Protection Agency, Washington, DC. 1991.
[2] World Health Organization. The World Health Report 2002; 2002.
[3] World Health Organization. Indoor air quality: organic pollutants; EURO report and studies, vol. 111. Copenhagen: WHO Regional Office for Europe; 1989.
[4] US EPA. Reducing risk: setting priorities and strategies for environmental protection; U.S. Washington, DC: Environmental Protection Agency; 1990.
[5] Chad B, Dorgan PE. Health and productivity benefits of improved indoor air quality. ASHRAE Transactions 1998;104(1):658–65.
[6] Meininghaus R, Salthammer T, Knoppel H. Interaction of volatile organic compounds with indoor materials—a small-scale screening method. Atmospheric Environment 1999;33:2395–401.
[7] Kim YM, Harrad S, Harrison RM. Concentrations and sources of VOCs in urban domestic and public microenvironments. Environmental Science and Technology 2001;35:997–1004.
[8] Sari DK, Kuwahara S, Tsukamoto Y. Effect of prolonged exposure to low concentrations of formaldehyde on the corticotropin releasing hormone neurons in the hypothalamus and adrenocorticotropic hormone cells in the pituitary gland in female mice. Brain Research 2004;1013(1):107–16.
[9] Fujishima A, Honda K. Electrochemical photolysis of water at a semiconductor electrode. Nature 1972;238:37–8.
[10] Tompkins DT. ASHRAE research project 1134-RP: evaluation of photocatalytic air cleaning capability: a literature review and engineering analysis. Final report; 2001.
[11] Zhao J, Yang XD. Photocatalytic oxidation for indoor air purification: a literature review. Building and Environment 2003;38(5): 645–54.

[12] Hall RT, Bendfeldt P, Obee TN, Sangiovanni JJ. Computational and experimental studies of UV/titania photocatalytic oxidation of VOCs in honeycomb monoliths. Journal of Advanced Oxidation Technology 1998;3:243–51.
[13] Zhang YP, Yang R, Zhao R. A model for analyzing the performance of photocatalytic air cleaner in removing volatile organic compounds. Atmospheric Environment 2003;37:3395–9.
[14] Yang R, Zhang YP. An improved model for analyzing the performance of photocatalytic oxidation reactor in removing volatile organic compounds and its application. Journal of Air and Waste Management Association 2004;54:1516–24.
[15] Mo JH, Zhang YP, Yang R. Novel insight into VOC removal performance of photocatalytic oxidation reactors. Indoor Air 2005;15(4):291–300.
[16] Hossain MM, Gregory BR, Hay SO, Obee TN. Three-dimensional developing flow model for photocatalytic monolith reactors. AIChE Journal 1999;45:1309–21.
[17] Frank PI, David PD. Fundamentals of heat and mass transfer, fourth ed; 1996. p. 731–35.
[18] Brucato A, Grisafi F, Urso R. Economic evaluation of photon sources for photocatalytic applications by means of spectral distribution analysis. International conference on TiO_2 photocatalytic treatment of water and air, Orlando, FL; 1997. 48pp.
[19] Obee TN. Photooxidation of sub-parts-per-million toluene and formaldehyde levels on titania using a glass-plate reactor. Environmental Science and Technology 1996;30:3578–84.